Available online at www.sciencedirect.com
ScienceDirect
Journal of Crystal Growth 310 (2008) 1366–1370
JOURNAL OF CRYSTAL GROWTH
www.elsevier.com/locate/jcrysgro

Numerical calculation of the drag force applied to particle pushing

E. Agaliotis[a,b,*], M.R. Rosenberger[a,b], C.E. Schvezov[a,b], A.E. Ares[a,b]

[a]CONICET (Consejo Nacional de Investigaciones Científicas y Técnicas), Rivadavia 1917, 1033 Buenos Aires, Argentina
[b]Prog. Materiales, Modelización y Metrología, FCEQyN, Universidad Nacional de Misiones, Azara 1552, 3300 Posadas, Misiones, Argentina

Available online 3 December 2007

Abstract

The interaction of solid particles with a solidifying interface is studied with numerical and analytical models for the drag and pushing forces. The numerical results of the drag force on a spherical particle and planar interface were compared with the forces given by both, the Stokes and modified Stokes equations. The pushing force was calculated employing the Casimir–Lifshitz–van der Waals force. The results show the range and degree of validity of the Stokes and modified Stokes equations for large and small separations.

From this, it is shown that the particle–interface separations for steady pushing obtained numerically, for the same particle radius and solidification velocity. In addition, the critical velocities obtained with the present hybrid model are compared with experimental results published in the literature.

PACS: 47.11.Fg; 47.10.ad; 81.10.Fq

Keywords: A1. Computer simulation; A1. Fluid flows; A1. Interfaces; A1. Particles; A1. Solidification

1. Introduction

The interaction of particles with a solidifying interface has been studied both experimentally and theoretically for many years. The first significant analytical models were developed in the 1950s and 1960s [1–13]. Several contributions have been published which introduced thermal effects [4,5,14,15]. In most cases, the drag force has been approximated by the modified Stokes equation. This equation is valid for a spherical particle and a planar interface and small separations between particle and interface. However, in most experimental cases, these conditions do not apply. In addition, the range and degree of validity of the modified Stokes equations has not been established with detail. In the present investigation, results of a numerical model for the drag is presented and compared with the forces given by the analytical equations. In addition, the separation distance for steady pushing and critical velocity for pushing is calculated and compared with experimental results. The advances will permit to develop a numerical model, which will include the thermal effects on the system particle–melt–solid.

2. Methods

2.1. Numerical model for the drag force

The physical problem, which is solved, consists of a spherical particle immersed in a liquid phase close to a planar solidifying interface. When steady pushing occurs, the separation distance between particle and interface is small compared to the particle radius and there are two opposing forces in equilibrium: the drag force and the repulsive or pushing force. The drag force is determined and analyzed using a numerical model employing the finite element method. The assumptions are that the particle moves in steady state ahead of a planar interface at a constant velocity, the gravity force is neglected, the fluid is Newtonian and the Reynolds number is much less than 1; an axial symmetry is also assumed. The domain is discretized using a quadrilateral non-structured mesh with second-order interpolation functions for the velocity field

*Corresponding author at: Prog. Materiales, Modelización y Metrología, FCEQyN, Universidad Nacional de Misiones, Azara 1552, 3300 Posadas, Misiones, Argentina.
E-mail address: eliana@fceqyn.unam.edu.ar (E. Agaliotis).

0022-0248/$ - see front matter © 2007 Elsevier B.V. All rights reserved.
doi:10.1016/j.jcrysgro.2007.11.188

and first order for the pressure field. The element equations were obtained using the Galerkin method and the system of equations was solved by the Picard method. The boundary conditions were no slip at the particle surface and a single with homogeneous velocity at the interface. The solid was modeled by assuming a very high viscosity.

3. Analytical methods

In order to compare the results of the drag force obtained with the numerical model, two analytical equations were used for large and small separations between particle and interface which are: the standard Stokes [1] and the modified Stokes [2–6] equations, respectively, which are given by the following equations;

$$F_{\mathrm{dStokes}} = 6\pi\mu V_{\mathrm{int}} R, \tag{1}$$

$$F_{\mathrm{dS-M}} = 6\pi\mu V_{\mathrm{int}} \frac{R^2}{h}, \tag{2}$$

where V_{int} is the interface velocity, μ the viscosity, R the particle radius and h the separation distance between particle and interface.

In addition, it is assumed that the repulsive force is the Casimir–Lifshitz–van der Waals force [6,7] given by

$$F_{\mathrm{r}} = \pi B_3 \frac{R}{h^2}, \tag{3}$$

where B_3 is a Casimir–Lifshitz–van der Waals constant. This force is employed to compare the predictions from the numerical and analytical models for the drag force and the critical velocity for pushing.

4. Results and discussion

The physical parameters for the melt used throughout the calculations correspond to a typical fluid with a viscosity of $1.5\times10^{-3}\,\mathrm{Pa\cdot s}$ and same density for particle and melt. A value of $B_3 = 1\times10^{-20}\,\mathrm{J}$ was employed in all cases. The model parameters were the particle radius R, the particle interface separation h, and the interface velocity V_{int}. The particle radius varied between 1 and 50 μm. The separation distance varied between h_{eq} and h_{min}, which correspond to the steady state of pushing and a minimum layer thickness of a melt that may be considered as a liquid, h_{min} was taken as $10^{-8}\,\mathrm{m}$ [16,17] and h_{eq} is estimated from Eq. (4) which is obtained from Eqs. (2) and (3):

$$h_{\mathrm{eq}} = \frac{B_3}{6\mu V_{\mathrm{eq}} R}. \tag{4}$$

A different mesh was employed for each separation distance between particle and interface. The range of velocities has a minimum value V_{c} for each physical condition, which was estimated using Eq. (5). Eq. (5) was obtained from Eq. (4) for $h_{\mathrm{eq}} = h_{\mathrm{min}}$

$$V_{\mathrm{c}} = \frac{B_3}{6\mu h_{\mathrm{min}} R}. \tag{5}$$

The results obtained in the finite element calculation were processed and compared with the analytical models. The comparison was made of the drag force, the steady pushing separation versus interface velocity (h_{eq} versus V_{int}) and critical velocity versus particle radius (V_{c} versus R).

5. Results for the drag force

The numerical results of drag force obtained from the finite element calculations F_{dSim} were compared with the corresponding analytical values given by Eqs. (1) and (2). For the comparison, following relations were employed: $F_{\mathrm{dSim}}/F_{\mathrm{dS-M}}$, $F_{\mathrm{dSim}}/F_{\mathrm{dStokes}}$ and $F_{\mathrm{dSim}}/F_{\mathrm{dSim}} = 1$, which correspond to a perfect correlation. The comparison was made in a range of relative separation $h/2R$ from 0.01 to 27.5.

The results shown in Fig. 1 have been obtained for a number of different conditions: a range of velocities, particle radius and separation distances between the particle and the solidification interface, which is simulated as a planar sink. Three particle radii were used in the calculations: 1, 10 and 50 μm. The separation distances employed were in a specific range for each particle radius as well as the particle–interface velocity, as shown in Table 1.

In the same Table, the estimated critical velocity obtained from Eq. (5) is listed where it is observed that

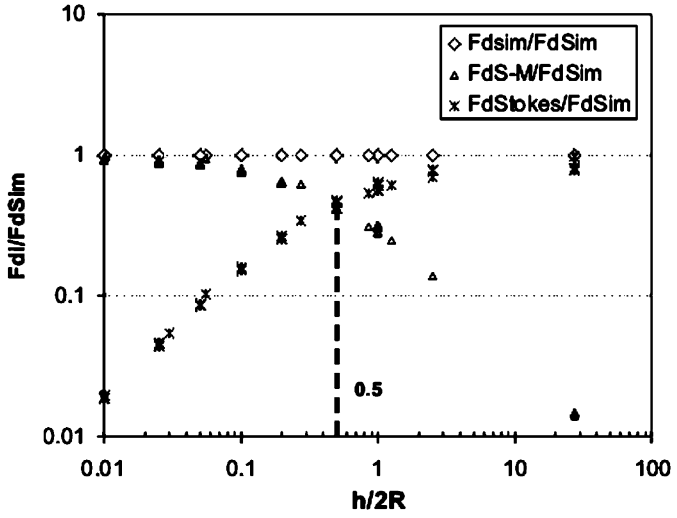

Fig. 1. Comparison of the finite element model results with the analytical values for the drag force.

Table 1
Values of the parameters used in the calculations

R (μm)	h (m)	V (m/s)	V_{c} (m/s)
1	1×10^{-8} to 5.5×10^{-5}	1.65×10^{-8} to 2.22×10^{-4}	1.11×10^{-4}
10	1.65×10^{-8} to 5×10^{-5}	1.65×10^{-9} to 2.22×10^{-5}	1.11×10^{-5}
50	1×10^{-8} to 1×10^{-4}	3.3×10^{-10} to 4.44×10^{-6}	2.22×10^{-6}

the largest velocity employed is twice the critical for each particle radius.

In addition, the calculations were done for different mesh configurations, number of elements and nodes. From the numerical modeling point of view, the most critical conditions are given for each end of the interval, which corresponds to the asymptote for large values of $h/2R$ and also the limit for small values of $h/2R$. In the first asymptote, and since in all cases, the boundary condition of a sink was applied, the discretization of the whole domain is necessary to obtain the last point in Fig. 1 for $h/2R = 27.5$; in this case, three different meshes were used with 43,629, 49,154 and 60,000 elements, respectively, which were not refined enough around the particle to obtain the same degree of accuracy of the other points. The given values in the figure are average values obtained from a number of conditions, with a minimum of seven values to a maximum of 21 values. The effort was focussed in the transition from the Stokes to the modified Stokes equations and also, for small values of $h/2R$ which correspond to the critical pushing conditions. From the results, it is observed that there is a large interval in which none of the approximations could be applied. The transition point which separates the best fit of each analytical approximation is $h/2R = 0.5$. In the case of small separations, it is observed that the numerical results fit very well to the analytical modified Stokes equation, for a significant range of velocities, which in the larger values, exceed twice the critical velocity.

6. Separation distance and critical velocity

The values of drag force obtained with the finite element method were used to determine the separation distance between the particle and the interface for different interface velocities and particle radius. The pushing force as explained above, correspond to the Casimir–Lifshitz–van der Waals force. The results are shown in Fig. 2. It is obtained that the equilibrium separation distance decreases with interface velocity linearly for both, large velocities and small separations up to a value of approximately 10^{-6} and with a slope around 45°. In addition, for a given velocity, the pushing separation distance decreases with increasing radius in the same way.

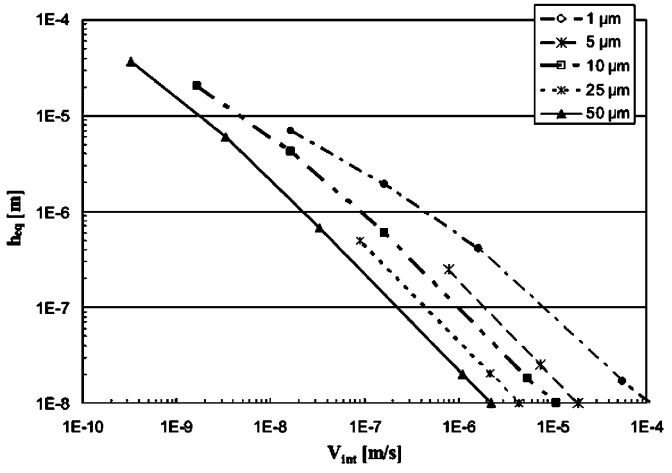

Fig. 2. Equilibrium separation for steady pushing for different particle radii obtained from the numerical model for the drag force.

When these results are compared with those predicted by the analytical model given by Eq. (4), it is obtained that in all the cases, the separation distance for steady pushing is always larger than the numerical model predictions. Indicating that larger particles could be pushed at higher velocities.

In order to find an empirical equation that could correlate the separation distance versus solidification velocity, three different functions were used to adjust the model results:

$$V_{\text{int}} = \frac{a_6}{h_{\text{eq}}^{b_6}}, \tag{6}$$

where a_6 and b_6 are functions of R given by the following equations:

$$a_6 = 1.083 \times 10^{-11} R^{-1.3518},$$
$$b_6 = 0.0457 \ln(R) + 0.767,$$

where R is given in μm. The second equation obtained is

$$V_{\text{int}} = \frac{a_7}{h_{\text{eq}}^{b_7} h_{\text{eq}}^{c_7 \log(h_{\text{eq}})}}, \tag{7}$$

where a_7, b_7 and c_7 are also functions of R given by the following equations:

$$a_7 = 1.64706 \ln(R) - 21.91879,$$
$$b_7 = 0.54163 \ln(R) - 3.67851,$$
$$c_7 = 0.035395 \ln(R) - 0.179956,$$

and finally the third equation is obtained from Eq. (4) as

$$V_{\text{int}} = \frac{B_3}{6\mu h_{\text{eq}} R}. \tag{8}$$

The results of the fitting of the three Eqs. (6)–(8) are shown in Fig. 3 for three different particle radii: 1, 10, and 50 μm.

Comparing the different models, it is observed that model 2 given by Eq. (6) is simpler than model 3 given by Eq. (7), however, as can be seen in Fig. 3(a)–(c), model 3 has a better fitting in the whole range of calculations. The factor $1/h_{\text{eq}}^{c_7 \log(h_{\text{eq}})}$ in Eq. (7) results to be an adjusting term of Eq. (6), which corrects the deviation for small particles. This factor tends to 1 for larger particles and Eqs. (6) and (7) become the same function given by Eq. (6). It is interesting to note that the three Eqs. (6)–(8) produce the same results for large velocities and, therefore, small separation distances; in Fig. 3(a)–(c), the lowest value of separation is 10^{-8} m which corresponds to the minimum separation for pushing; that is, gives the critical velocity for pushing for each particle radius. In this case, any of the three equations gives a good relation between critical velocity as a function of particle radius. For simplicity,

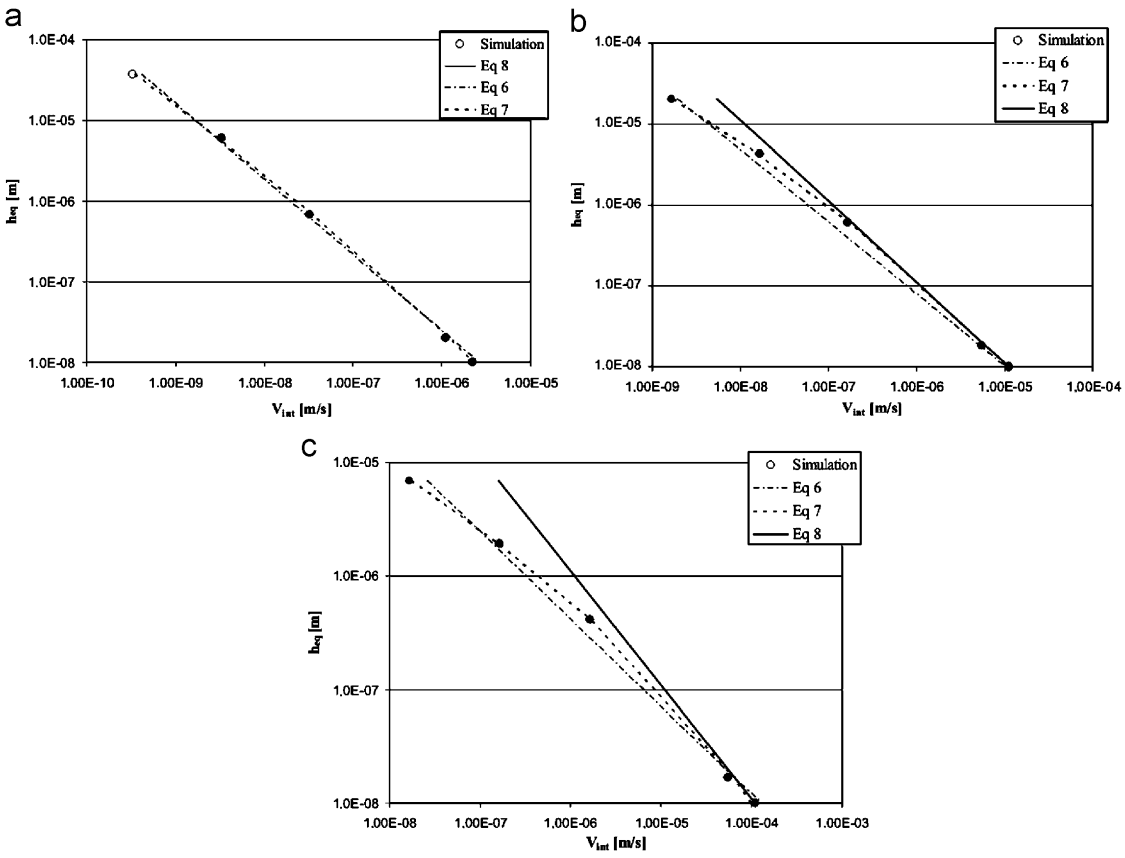

Fig. 3. Results of the fitting of h_{eq} versus V_{eq} using Eqs. (6)–(8) for three radii: (a) 50 μm, (b) 10 μm and (c) 1 μm.

Eq. (8) may be chosen as a good approximation to predict critical velocity for pushing and compare with experimental results. It is noted that experimentally, the critical velocity for pushing is observable which is measured and reported in the literature [4,18–23]. Moreover, most of the experiments were made using water as solidifying material and different particle materials. In view of this, the critical velocities for pushing, predicted by Eq. (8), with $h_{eq} = 10^{-8}$ m are compared with experimental results in water. The results are shown in Fig. 4.

It is first observed that the scattering in the experimental values is high, and second that Eq. (8) gives a good estimation of critical velocity as a function of particle radius. The scattering around the line given by Eq. (8) is estimated as

$$\log(V_{cm})_i \pm A^*, \tag{9}$$

where $(V_{cm})_i$ is the predicted value at each radius and $A^* = \text{average}[\log(V_{c,max})_i - \log(V_{c,min})_i]$.

In which, $(V_{c,max})_i$ and $(V_{c,min})_i$ are the maximum and minimum value of experimental velocity reported at each radius. The data for SiO_2 [4] and Pyrex [18] are not considered due to the anomalities. The parameters A^* as well as $\log(V_{cm})_i$ are listed in Table 2.

The logarithmic dispersion A^* in Table 2 shows the largest value of approximately 0.43 for the lower radius.

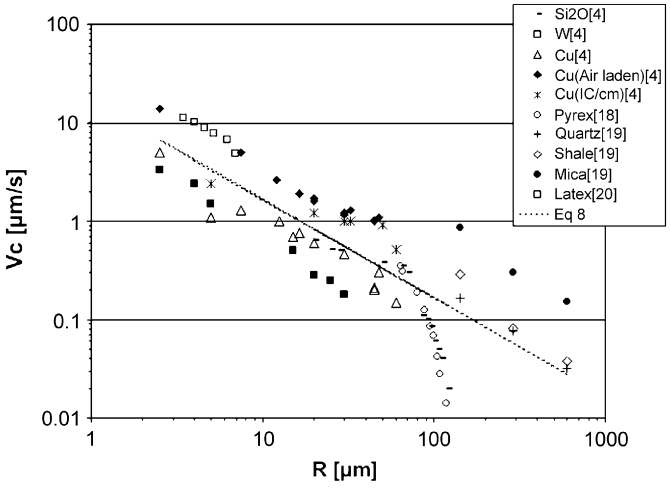

Fig. 4. Critical velocities for pushing in water, comparison between experiments and model.

The experimental scatter cannot be associated to the particle thermal properties of the material since the scatter occurs for metallic materials as well as for ceramic materials. It could be associated to the particle shape and also to the effect of the particle material on the pushing force, since it is observed that for two metals like tungsten and copper, the first have critical velocity consistently

Table 2
Values of A^* and $\log\left(V_{cm}\right)_i$ corresponding to Eq. (9)

R (μm)	A^*	$\log\left(V_{cm}(\mu m/s)\right)_i$
2.5	0.313807	0.823910
5	0.429335	0.522880
30	0.429335	−0.255272
50	0.282136	−0.454844
291	0.298191	−1.242043

below the model prediction and the second above the prediction. The discrepancy of the experimental results reported for SiO_2 [4] and Pyrex [18] with the other materials could be the result of a more complex interaction in the system particle-melt-solid. Nevertheless, Eq. (8), for most of the experimental results shown in Fig. 4, may be considered a good first approximation to predict the critical velocity for pushing for a given particle radius.

7. Summary and conclusions

The drag force for an spherical particle during solidification has been calculated numerically in a range of particle radius between 1 and 50 μm and separation distances between particle and interface from 1×10^{-8} m to 1×10^{-4} m.

The results have been compared with the drag force given by the Stokes and modified Stokes equations and show the following:

- The numerical calculations give values which are consistently larger than the analytical calculations.
- The modified Stokes equation could be used as a good approximation in the range of values of $h/2R$ between $h_{min}/2R$ and $h/2R<0.5$.

In addition, the numerical and analytical drag forces were compared with the pushing force given by the Casimir–Lifshitz–van der Waals force, resulting in two fitted relations between the equilibrium separation distance h_{eq} between particle and solidifying interface and its velocity V_{eq} as

$$V_{eq}=\frac{a}{h_{eq}^{b}}, \tag{10}$$

$$V_{eq}=\frac{a}{h_{eq}^{b}h_{eq}^{(c\log(h_{eq}))}}. \tag{11}$$

The comparison of the critical velocity predicted by Eqs. (6) and (7) as a function of particle radius with experimental values reported for water and a number of different particles indicate that Eqs. (6) and (7) are first good approximations to predict critical velocities for pushing as a function of particle radius.

Acknowledgment

The authors acknowledge the support from CONICET (Consejo Nacional de Investigaciones Científicas y Técnicas), Argentina.

References

[1] R.L. Daugherty, A.C. Ingersoll, Mecánica de los fluidos (1964) 348.
[2] E. Dzyaloshinskii, E.M. Lifshitz, L.P. Pitaevskii, General theory of van der Waals forces, Sov. Phys. USPEKHI 72 (1961) 153–176.
[3] D.R. Uhlmann, B. Chalmers, K.A. Jackson, Interaction between particles and a solid–liquid interface, J. Appl. Phys. 35 (1964) 2986.
[4] J. Cisse, G.F. Bolling, A study on the trapping and rejection of insoluble particles during the freezing of water, J. Crystal Growth 10 (1971) 67.
[5] G.F. Bolling, J. Cisse, A theory for the interaction of particles with a solidifying front, J. Crystal Growth 10 (1971) 56.
[6] A.A. Chernov, D.E. Temkin, S.M. Mel'nikova, Theory of the capture of solid inclusions during the growth of crystals from the melt, Sov. Phys. Crystallogr. 21 (4) (1976) 369.
[7] P. Casses, M.A. Azouni-Aidi, A general theoretical approach to the behavior of foreign particles at advancing solid–liquid interfaces, Adv. Colloid Interface Sci. 50 (1994) 103–120.
[8] M.V. Pikunov, The Behavior of Suspended Impurities During Crystallization. Non Ferous Metals, Their Treatment and Working, Metallurgizdat, Moscow, 1957, p. 56.
[9] A.W. Neumann, D.J. van Oss, J. Szekely, Thermodynamics of particle engulfment, Kolloid Z.U.Z. Polymere 251 (1973) 415.
[10] S.N. Omenyi, A.W. Neumann, Thermodynamic aspects of particle engulfment by solidifying melts, J. Appl. Phys. 47 (1976) 3956.
[11] A.M. Zubko, V.G. Lobanov, V.V. Nikonova, Reaction of foreign particles with a crystallization front, Sov. Phys. Crystallogr. 18 (2) (1973) 239.
[12] M.K. Surappa, P.K. Rohatgi, Heat diffusivity criterion for the entrapment of particles by a moving solid–liquid interface, J. Mater. Sci. 16 (2) (1981) 562.
[13] C.E. Schvezov, F. Weinberg, Interaction of iron particles with a solid–liquid interface in lead and lead-alloys, Metall. Trans. (USA) 16B (1985) 367.
[14] D. Shangguan, S. Ahuja, D.M. Stefanescu, An analytical model for the interaction between an insoluble particle and an advancing solid–liquid interface, Metall. Trans. A 23 (1992) 669.
[15] J.W. Garvin, H.S. Udaykumar, Drag on a particle being pushed by a solidification front and its dependence on thermal conductivities, J. Crystal Growth 267 (2004) 724.
[16] K.V. Sharp, R.J. Adrian, Transition from laminar to turbulent flow in liquid filled microtubes, Exp. Fluids 38 (1) (2005).
[17] K. Travis, B. Tood, D. Evans, Departure from Navier–Stokes hydrodynamics in confined liquids, Phys. Rev. E 55 (1997) 4288.
[18] P. Hoekstra, D.R. Miller, On the mobility of water molecules in the transition layer between ice and a solid interface, J. Colloid Interface Sci. 25 (1967) 166.
[19] A.E. Corte, Vertical migration of particles in front of a moving freezing plane, J. Geophys. Res. 67 (3) (1962) 1085.
[20] C. Körber, G. Rauy, M.D. Cosman, E.G. Cravalho, Interaction of particles and a moving ice–liquid interface, J. Crystal Growth 72 (1985) 649.
[21] C.E. Schvezov, Dynamic calculations for particle pushing, in: W.H. Hofmeister, J.R. Rogers, N.B. Singh, S.P. Marsh, P.W. Vorhes (Eds.), Solidification, TMS, USA, 1999, p. 251.
[22] C.E. Schvezov, Interaction of particles with an advancing solid/liquid interface, Master of Applied Science Thesis, Department of Metals and Materials Engineering, UBC, Canada, 1983.
[23] C.E. Schvezov, F. Weinberg, Interaction of particles with an advancing solid–liquid interface, in: Proceedings of the 33rd Canadian Metal Physics Conference, Kingston, Ont., Canada, June 1983.